Journal of Food Engineering 288 (2021) 110141

Contents lists available at ScienceDirect

Journal of Food Engineering

journal homepage: http://www.elsevier.com/locate/jfoodeng

# Heat and mass transfer of scraped surface heat exchanger used for suspension freeze concentration

Zhongxiang Ding [b], Frank G.F. Qin [a,*], Kewen Peng [a], Jiaojiao Yuan [a], Simin Huang [a], Runhua Jiang [a], Youyuan Shao [a]

[a] Institute of Chemical Engineering and Energy Technology, Dongguan University of Technology, Dongguan City, 523808, China
[b] School of Chemical Engineering and Light Industry, Guangdong University of Technology, Guangzhou, 510000, China

ARTICLE INFO

*Keywords:*
Multi-pass freeze concentration
Apple juice
Suspension crystallization
Modeling
Heat and mass transfer
Scraped surface heat exchanger

ABSTRACT

Freeze concentration (FC) by suspension crystallization is a complex process due to the combination of a scraped-surface heat exchanger, crystallizer, and wash column. Following the study of a three-in-one structure of a multi-pass FC published earlier this year, modeling and experiments of the heat and mass transfer of this freeze concentrator are presented in this paper. The experimental assessment of the system performance, including the measured values of the heat transfer coefficient, ice production rate, and energy efficiency as well as their correlation with the concentration ratio and partition coefficient are presented in this article.

## 1. Introduction

Freeze concentration (FC) is a nonthermal processing technology of liquid food, in which a portion of the water in the aqueous solution is frozen and converted into relatively pure ice crystals, after which it is removed from the liquid phase to concentrate the remaining solution. It can be used to concentrate or pre-concentrate heat-sensitive aqueous solutions, such as milk (Habib and Farid, 2007; Sanchez et al., 2011), fresh fruit juices (Orellana-Palma et al., 2017; Petzold et al., 2013; Bayindirli et al., 1993), other liquid foods (Moreno et al., 2014a), and biological solutions (Moreno et al., 2014b). Studies have shown that compared with evaporation concentration, FC has the advantage of producing less thermal denaturation of the solution, and thus, it can better maintain the original flavor, nutrition, and color of liquid foods (Benedetti et al., 2015; Moreno et al., 2014c; Miyawaki et al., 2016a). Moreover, the latent heat of water freezing is almost one seventh of the latent heat of water evaporation (Lide and Haynes, 2010), which offers potential for energy savings for de-watering of aqueous solutions.

Ice crystals can be formed from aqueous solutions in two ways: progressive crystallization (Miyawaki et al., 2005, 2016b; Zambrano et al., 2018) and suspension crystallization (Huige and Thijssen, 1972; Qin et al., 2007). In the former, the water freezes on the cooling surface, forming an ice layer progressively and a concentrated liquid phase. Thus, it is also known as layer crystallization. This method of FC is called progressive FC. When the ice layer extends to the entire vessel to form an ice block, it is known as block FC (Moreno et al., 2014c; Zambrano et al., 2018). The advantage of this technology is the low equipment cost and simple operation management. However, the ice layer has a poor heat transfer coefficient of less than 0.1 kW $m^{-2}$ $K^{-1}$ (Qin et al., 2003a; Pronk et al., 2010; Hasan et al., 2017), and a huge cooling surface area is required for practical applications. In addition, the ice layer tends to entrain liquid sacs and causes severe solute loss (Miyawaki et al., 2016a, 2016b; Samsuri et al., 2015).

In the latter method, a scraped-surface heat exchanger (SSHE) is used to clean ice scaling from the cooling surface and improve the heat transfer coefficient, the value of which is correlated to the speed of the scraper and the solution concentration and varies between 200 and 1000 W $m^{-2}$ $K^{-1}$, corresponding to a specific ice production rate up to 40 kg $h^{-1}$ $m^{-2}$ (Qin et al., 2003b, 2016; Abichandani et al., 1987; Rao and Hartel, 2006). However, the newly formed ice crystals are very small and must undergo Ostwald ripening for efficient solid-liquid separation (Pronk et al., 2005; Thijssen and Spicer, 1974; Qin et al., 2008). The ice crystals will be compressed into a close-packed ice bed and then separated with the mother liquor in a wash column (wash tower) (Schwartzberg et al., 1990). This process and its equipment are complex, and the costs of investment and maintenance are high, which hinders its application. Therefore, it is believed that future research and development in the field of freeze concentrators should focus on novel crystallizer design, to reduce equipment costs and increase the process efficiency, as well as efficient cooling methods, with an emphasis on a single unit operation that incorporates both crystallization and

* Corresponding author.
*E-mail address:* qingf@dgut.edu.cn (F.G.F. Qin).

https://doi.org/10.1016/j.jfoodeng.2020.110141
Received 30 December 2019; Received in revised form 3 May 2020; Accepted 14 May 2020
Available online 16 May 2020

**Nomenclature**

| | |
|---|---|
| $A$ | cooling surface area ($m^2$) |
| $C$ | juice concentration °Bx or [g (100 g)$^{-1}$] |
| $cp$ | specific heat capacity (kJ kg$^{-1}$ °C$^{-1}$) |
| $F$ | blade number of the rotational scraper |
| $f$ | mass fraction of ice or crystallinity (%) |
| $\Delta H$ | latent heat of water freezing (= 334 kJ kg$^{-1}$) |
| $hil$ | individual heat transfer coefficient between liquid and solid wall of the cooling surface (W m$^{-2}$ °C$^{-1}$) |
| $In$ | nth-order modified Bessel functions of the first kind |
| $Kn$ | nth-order modified Bessel functions of the second kind |
| $\kappa$ | variable defined for the treatment of the original partial differential equation |
| $kis$ | rate constant of ice formation on the cooling surface, which is defined as the ice pro-duction rate per square meter of cooling surface per degree of supercooling (kg s$^{-1}$ m$^{-2}$ °C$^{-1}$) |
| $M$ | mass (kg) |
| $n$ | rotational speed of the scraper (rpm) |
| $p$ | partition coefficient |
| $Q$ | heating or cooling capacity (kJ) |
| $r$ | concentration ratio |
| $Tb$ | bulk solution temperature (K or °C) |
| $Tc$ | coolant temperature (K or °C) |
| $Tf$ | freezing point of aqueous solution (°C) |
| $t$ | freezing time, i.e., ice crystallization time (s) |
| $\Delta Tw$ | wall supercooling (K or °C) |
| $U$ | overall heat transfer coefficient (W m$^{-2}$ °C$^{-1}$) |
| $v$ | transverse growth speed of ice film spreading alongside on the cooling surface (μm s$^{-1}$) |
| $Vi$ | volume of ice ($m^3$) |
| $w$ | ice production rate (kg h$^{-1}$ m$^{-2}$) |
| $y$ | soluble solid recovery yield (%) |
| $\delta$ | thickness of the newly formed ice film at the growing front (m) |
| $\phi$ | ratio of the ice-free area to the entire scraped-cooling-surface area ($0 \leq \phi \leq 1$) |
| $\lambda l$ | thermal conductivity of liquid (J m$^{-1}$ °C$^{-1}$) |
| $\rho l$ | density of liquid (kg m$^{-3}$) |
| $\rho i$ | density of ice (kg m$^{-3}$) |

*Subscripts*

| | |
|---|---|
| 0 | original juice before freeze concentration |
| 1, 2, 3 | 1st, 2nd, and 3rd passes of freeze concentration |
| $i, j$ | ice and juice, respectively |
| $s$ | soluble solid in juice |
| $w$ | water in juice |

separation in one piece of equipment (Randall and Nathoo, 2015). This requires a comprehensive understanding and modeling of the process of suspension FC, including the heat and mass transfer of the SSHE, the correlation of the ice production rate with the system cooling, and the recovery yield of the soluble solid with ice crystallization.

Moreover, a common concentration scenario, such as to concentrate a dilute solution from 10 to 20°Bx (or higher), requires a dehydration of 50% (or even more). When such an amount of water is converted into ice crystal particles, ice actually fully fills the whole crystallizer and leaves concentrated liquid between the ice particles (Qin et al., 2009a), which deteriorates the heat and mass transfer quickly. The ice must be removed from the concentrated mother liquor to achieve a higher concentration. The de-watering requirements for concentrating a 10°Bx aqueous solution to a higher concentration are shown in Table 1, which indicates that when a final concentration of more than 20°Bx is required, more than one batch operation is required unless a continuous crystallization and separation method is used.

To address the above problems, a three-in-one FC structure was proposed, in which the SSHE, crystallizer, and wash-column were united in a single piece of equipment, and multi-pass (batch) suspension crystallization was applied to achieve a higher product concentration (Ding et al., 2019; Qin et al., 2019). A screw scraper was further used in the SSHE. Most of the previous studies on SSHEs were based on straight-blade scrapers. Information on screw-scraper SSHEs is lacking, especially for ice production. This study focused on the modeling and experiments of the heat and mass transfer of a FC system using screw-scraper SSHE.

The juice (raw material) used in this study was "Huiyuan Youth 100% Apple Juice," which was available in 1-L packs in the local market, with a concentration of 10.5°Bx.

**Table 1**
De-watering requirements for concentrating a 10°Bx aqueous solution.

| Desired concentration (°Bx) | 10 | 20 | 30 | 40 | 50 | 60 | 70 |
|---|---|---|---|---|---|---|---|
| Water to be removed (% w/w) | 0 | 50.00 | 66.67 | 75.00 | 80.00 | 83.33 | 85.71 |

## 2. Experimental apparatus and procedure

The experimental system was basically the same as that described in our previous paper with minor modifications. It mainly consisted of a refrigeration unit, a scraper heat exchanger, a crystallizer, a measurement and control unit, and two storage tanks (Ding et al., 2019). The SSHE, an important part of the FC system that is associated with the heat and mass transfer, used a screw scraper, as shown in Fig. 1. The scraper not only provided scraping action on the cooling surface but also helped to drive ice and juice to float upward into the suspension crystallizer located above. When the juice was cooled to or below its freezing point, dendritic nuclei of the ice precipitated on the cooling surface first (Qin et al., 2009b), which was then scraped off to mix with the solution to form an ice slurry. The ascending ice crystals were intercepted by the perforated plate below the top cover of the crystallizer, but the juice passed through the perforated plate and flowed out of the top cover and returned to the bottom of the SSHE to form external circulation. The process flowchart is shown in Fig. 2, where the pre-treatment steps were completed by the juice manufacturer, and the freeze concentration steps were carried out using the experimental setup described above.

During the ice production period, i.e., the freezing stage, ice Ostwald ripening occurred in the crystallizer simultaneously, which required at least for 3 h for dilute aqueous solutions, such as the original apple juice at a concentration of approximately 10°Bx (a higher juice concentration requires longer ripening times). During this time, newborn micron-size dendritic ice nuclei grew to several hundreds of microns to make the final washing operation possible. When the crystallizer was fully filled by ice particles and formed a tightly packed ice bed, freezing of the pass-1 FC ended and was followed by a wash process, in which 0 °C water was introduced into the crystallizer from the top cover to displace the concentrated juice of the ice bed in a form of plug flow. The concentrated juice was discharged at the bottom of the SSHE simultaneously. The same volume of water as that of the concentrated juice collected was added. The flow rate was controlled under the critical velocity to maintain plug-flow in the ice bed, which produced a sharp wash front, or interface, between the washed and un-washed ice beds. This prevented

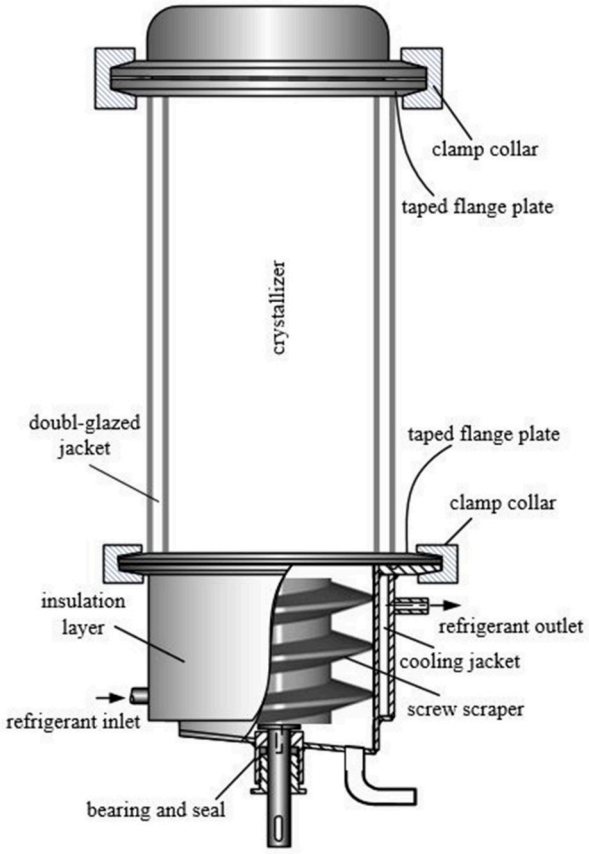


**Fig. 1.** Anatomy of the scraped-surface heat exchanger.

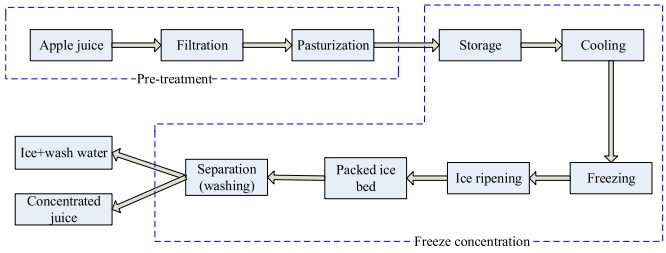


**Fig. 2.** Flowchart outlining the freeze concentration process used in this study.

the mixing of water and the concentrated juice. The concentration of the latter was approximately 1.8 times that of the original juice. If targeting a higher concentration, the collected pass-1 FC juice would sent through a second FC process, which is referred to as the pass-2 FC, and so on. For more details of the FC system and experimental procedure, please refer to our previous published articles (Ding et al., 2019; Qin et al., 2019).

## 3. Modeling and calculation methodology

### 3.1. Heat and mass transfer of the SSHE

FC of dilute aqueous solutions is a mass transfer process driven by heat transfer. Only when the latent heat released by water crystallization is continuously extracted from the solution (heat transfer) through the SSHE and refrigeration unit can the crystallization of water be sustainable (mass transfer). According to Qin et al., 2003b, 2009b, the heat transfer process on the cooling surface of the solution phase can be divided into three stages, as shown in Fig. 3. In stage I, the heat flux occurred from the solution to the cooling surface, during which the solution was cooled without phase change. In stage II, when the solution temperature was equal to or below its freezing point, phase change began, ice crystal nuclei appeared, the latent heat of phase change on the cooling surface was released, and the temperature of the solution jumped to the phase equilibrium point (freezing point). This stage was extremely short, only lasting a few seconds. Therefore, in the graph of temperature vs. FC time, the temperature rise was a vertical straight line. In stage III, the ice crystals continued to form on the cooling surface and were scraped off. The juice temperature decreased slowly because of the freezing point depression (FPD). Stages II and III are known as freezing stages.

Since the refrigerant was in boiling state in the cooling jacket with a high heat transfer coefficient, the main heat transfer resistance occurred on the solution side. On the cooling surface of the SSHE, the individual heat transfer coefficient of the solution can be expressed as follows:

$$h_{il}=\begin{cases}\left(\dfrac{\lambda_l\rho_l c_{pl}nF}{15\pi}\right)^{1/2}, & \text{(cooling stage I)}\\ k_i\Delta H+\varphi\left(\dfrac{\lambda_l\rho_l c_{pl}nF}{15\pi}\right)^{1/2}, & \text{(freezing stage II \& III)}\end{cases} \tag{1-2}$$

where $k_i$ is the constant of the ice formation rate on the subcooled surface (kg m$^{-2}$ °C$^{-1}$ s$^{-1}$); $\Delta H$ is the latent heat of freezing, which is 334.11 kJ kg$^{-1}$ for water; $\lambda_l$, $\rho_l$, and $c_{pl}$ are the thermal conductivity (J m$^{-1}$ °C$^{-1}$ s$^{-1}$), density (kg m$^{-3}$), and specific heat (kJ kg$^{-1}$ °C$^{-1}$) of the liquid, respectively; $n$ and $F$ are the rotational speed (rpm) and blade number of the scraper, respectively; $\phi$ is the ratio of the ice-free area to the entire scraped-surface area ($0 \le \phi \le 1$). The individual heat transfer coefficient was independent of the time ($t$), but it depended on the state of the solution, cooling, or freezing.

In the stage of ice nucleation, i.e., stage II, nuclei appeared on the cooling surface at randomly distributed points. If they were not scraped off, they tended to spread along the cooling surface until covering the entire surface and forming a thin layer of ice. This process was driven by heat transfer. The spreading growth kinetics equation of the ice film can be expressed as follows (Qin et al., 2004):

$$\frac{K_1(\kappa v\delta)\cdot I_0(-\kappa v\delta)}{K_0(\kappa v\delta)}+I_1(-\kappa v\delta)-\frac{\rho\Delta H}{\pi\lambda\kappa\Delta T_w}=0 \tag{3}$$

where $I_0$ and $I_1$ are the zero- and first-order modified Bessel functions of the first kind, respectively, $K_0$ and $K_1$ are the zero- and first-order modified Bessel functions of the second kind, respectively, $\kappa$ is a variable defined for solving the original partial differential equation, $\delta$ is the thickness of the ice film, $v$ is the transverse growth speed of the ice film spreading alongside the cooling surface.

The ice film would continue to thicken into a macroscopic visible ice layer if it failed to be scraped off, and thus, it is known as layer

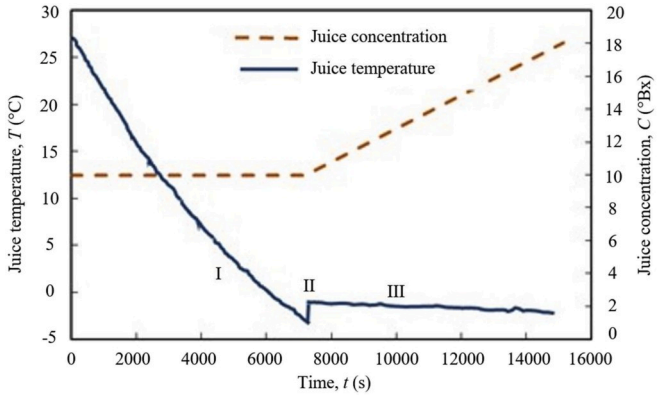


**Fig. 3.** Temperature and concentration changes over time in suspension FC (Ding et al., 2019).

crystallization or progressive crystallization. After this point, the individual heat transfer coefficient would no longer be independent of time ($t$), as shown in Eqs. (1) and (2), but it would decline proportionally to $1/\sqrt{t}$ (Qin et al., 2003b):

$$\overline{h}_l = 2\left(\frac{\lambda_l \rho_l C_p}{\pi t}\right)^{1/2} \tag{4}$$

where $t$ is the freezing time.

### 3.2. Correlation of ice production with concentration ratio (r), partition coefficient (p), mass fraction of ice (f), and recovery yield (y)

Ice production is a result of the heat and mass transfer of the SSHE, so the heat and mass transfer affect the concentration ratio, partition coefficient, and ice mass fraction. The content of soluble solids in liquid foods, e.g., fruit juice, is often referred to as the weight concentration, which is defined as follows:

$$C_j = \frac{100 M_s}{M_w + M_s} \tag{5}$$

where $M_s$ is the mass of the soluble solid, $M_w$ is the mass of the water in the juice solution, and $C_j$ is the weight concentration in terms of °Bx (grams per 100 g of solution). The main soluble solid component of the apple juice was sugar. The definition of the Brix degree (°Bx) is based on sucrose (grams of sucrose per 100 g of sucrose solution at 20 °C). In this study, we used a refractometer to measure the juice concentration, so the concentrations of apple juice are presented in °Bx. Since there were small amounts of other soluble substances in the juice, using °Bx approximates the weight concentration (% w/w).

When a small amount of water ($dM_w$) froze and became ice, the concentration had a gain of $dC_j$ due to the decrease in the amount of solvent, i.e. water, in the solution. The derivative of $C_j$ (Eq. (5)) with respect to $M_w$ is as follows:

$$\frac{dC_j}{dM_w} = -\frac{100 M_s}{(M_w + M_s)^2} \tag{6}$$

We assumed that the content of soluble substances remained constant and the ice was pure. The latter is valid when ice particles grow by Ostwald ripening under conditions close to phase equilibrium. This was verified by determining the low-soluble-solid content in ice in our previously published article (Ding et al., 2019). Since the decrease in water content in the solution was equal to the increase in the amount of ice based on a mass balance, but with opposite sign, we have the following:

$$M_w = M_{w0} - M_i \text{ and } dM_w = -dM_i \tag{7}$$

where $M_{w0}$ is the initial water mass in the original juice solution, and $M_i$ is the mass of ice.

Substituting Eq. (7) into Eq. (6) for the pass-1 FC, integrating with respect to $C_j$ from $C_{j0}$ to $C_{j1}$ on the left-hand side and integrating with respect to $M_i$ from 0 to $M_{i1}$ on the right-hand side yields the following:

$$\int_{C_{j0}}^{C_{j1}} dC = 100 M_s \int_0^{M_{i1}} \frac{dM_i}{(M_{w0} + M_s - M_i)^2} \tag{8}$$

$$C_{j_1} - C_{j0} = \frac{100 M_s}{M_{w0} + M_s - M_i} - \frac{100 M_s}{M_{w0} + M_s} \tag{9}$$

According to the concentration definition of Eq. (5), the initial concentration of the juice solution is written as follows:

$$C_{j0} = \frac{100 M_s}{M_{w0} + M_s} \tag{10}$$

The mass balance of the soluble solids of the original juice, concentrate, and ice can be written as follows:

$$M_{j0} = M_{j1} + M_{i1} \tag{11}$$

where $M_{j0}$ is the mass of the original juice, and $M_{j1}$ and $M_{i1}$ are the mass of the juice concentrate and ice at the end of the pass-1 FC, respectively. Substituting Eqs. (10) and (11) into Eq. (9) and reorganizing yields the following:

$$\frac{M_{i1}}{M_{j0}} = 1 - \frac{C_{j0}}{C_{j1}} \tag{12}$$

Eq. (12) correlates the mass fraction of ice $M_{i1}/M_{j0}$ with the concentration ratio $C_{j0}/C_{j1}$ of the pass-1 FC. We used concentration ratio ($r$) to denote the concentration increase, which is the ratio of juice concentration after FC ($C_{j1}$) and before FC ($C_{j0}$):

$$r_1 = \frac{C_{j1}}{C_{j0}} \tag{13}$$

The partition coefficient (also known as the distribution coefficient/constant) (Miyawaki et al., 2005, 2016b) to express the entrainment of soluble solid by ice is as follows:

$$p_1 = \frac{C_{i1}}{C_{j1}} \tag{14}$$

where $C_{i1}$ is the soluble solid content in the ice, and $C_{j1}$ is the soluble solid concentration of the concentrated mother liquor. The subscripts $i$ and $j$ denote the ice and juice, respectively, and the subscript 1 represents the first pass of FC. This subscript convention is used hereinafter. The fraction of ice crystal mass out of the original juice mass is called the ice crystal mass fraction or the crystallinity of the original juice of the first pass:

$$f_1 = \frac{M_{i1}}{M_{j0}} \tag{15}$$

The mass ratio of the soluble solid between the concentrated and original juice is called the recovery yield:

$$y_1 = \frac{M_{j_1} C_{j1}}{M_{j0} C_{j0}} \tag{16}$$

Based on the mass balance, the mass of the soluble solid in the original juice, concentrate, and ice can be written as follows:

$$M_{j0} C_{j0} = M_{j1} C_{j1} + M_{i1} C_{i1} \tag{17}$$

Therefore, in the pass-1 FC, the process recovery yield ($y_1$) can be represented by the mass fraction of ice ($f_1$), the partition coefficient ($p_1$), and the concentration ratio ($r_1$):

$$\begin{aligned} y_1 &= \frac{M_{j1} C_{j1}}{M_{j0} C_{j0}} = \frac{M_{j0} C_{j0} - M_{i1} C_{i1}}{M_{j0} C_{j0}} = 1 - \frac{M_{i1} C_{i1}}{M_{j0} C_{j0}} \\ &= 1 - \frac{M_{i1}}{M_{j0}} \cdot \frac{C_{i1}}{(C_{j1}/r_1)} = 1 - f_1 p_1 r_1 \end{aligned} \tag{18}$$

For the same argument, the above formulas can be applied to the pass-2 and pass-3 FC, in which the subscript 1 will be replaced by 2 and 3, respectively.

### 3.3. Ice production rate of system

The specific ice production rate, or simply the ice production rate (used hereinafter), refers to the mass of ice crystals produced per unit time per unit cooling area. Since the ice mass cannot be directly measured on-line in the system, it is reflected in the change of juice concentration. In pass 1, the juice concentration can be obtained by multiplying the two sides of Eq. (12) by ($M_{j0}/At$) simultaneously:

$$w_1 = \frac{M_{i1}}{At} = \left(1 - \frac{C_{j0}}{C_{j1}}\right) \frac{M_{j0}}{At} \tag{19}$$

where $t$ is the time from the initial to the final freezing points (ice crystallization), $M_{j0}$ is the mass of the original juice, $C_{j0}$ is the initial

concentration of the juice before FC, and $C_{j1}$ is the concentration of the juice after FC. Thus, Eq. (19) provides a method to measure the ice production rate, where the mass of the original juice, $M_{j0}$, can be obtained by weighing, and the juice concentration, $C_{j1}$, can be measured by determining the freezing point temperature or using a refractometer. The cooling area, $A$, is fixed in the system, and the freezing time is recorded by the control unit. In the scraped surface heat exchanger, freezing of the juice solution occurs at the phase equilibrium temperature (freezing point), and thus, the freezing point depression (FPD) can be used to determine the juice concentration. The equation of the apple juice FPD (temperature) that was published in our previous article was used, which is as follows (Ding et al., 2019):

$$C_j = -0.0014T_f^4 - 0.0626T_f^3 - 1.071T_f^2 - 10.398T_f \tag{20}$$

where $C_j$ is the apple juice concentration, and $T_f$ is the temperature of the apple juice at the freezing time, which is equivalent to the freezing point of the juice.

The reason that we did not weigh the ice column to obtain the ice mass is because the ice column after being washed is a mixture ice and fresh water rather than being ice only. Eq. (19) is also applicable to the calculation of the ice production rates for passes 2 and 3.

### 3.4. Heat transfer coefficient of SSHE (U)

In the initial cooling stage of the FC process, i.e., stage I found in Fig. 3, there was no phase change in the juice before its temperature dropped to or below the freezing point. The sensible heat released by the fruit juice due to cooling was equal to the heat carried away by the refrigerant. According to the analysis given by Qin et al., the heat transfer coefficient $U_{\mathrm{I}}$ of the SSHE in this stage was determined as follows (Qin et al., 2003b, 2009b):

$$U_{\mathrm{I}} = \frac{c_p M_{j0}}{A t_{\mathrm{I}}} \ln\left(\frac{T_{b1} - T_c}{T_{b2} - T_c}\right) \tag{21}$$

where $c_p$ is the specific heat capacity of the fruit juice, $A$ is the cooling surface area, which was 0.0314 $m^2$ in this freeze concentrator, $t_{\mathrm{I}}$ is the time required for the juice temperature to drop from the initial room temperature to its freezing point, i.e., the duration of stage I, $T_{\mathrm{c}}$ is the refrigerant temperature, and $T_{b1}$ and $T_{b2}$ are the temperatures at which the fruit juice began to cool and at which the cooling stage was terminated, respectively. Eq. (21) is the basis for measuring the heat transfer coefficient of the cooling stage, $U_I$.

In the nucleation and ice production stages of the FC, i.e., stages II and III, according to Eq. (12), the ice crystal mass $M_{i1}$ can be obtained from the mass $M_{j0}$ of the original juice and the concentration change caused by the ice formation. The latent heat released by the water freezing (phase change) with an ice mass of $M_{i1}$ is as follows:

$$Q = M_{i1}\Delta H = M_{j0}\Delta H\left(1 - \frac{C_{j0}}{C_{j1}}\right) \tag{22}$$

where $\Delta H$ is the latent heat of freezing (kJ $kg^{-1}$).

According to Fourier's law of heat transfer, the heat carried away by the refrigerant of temperature $T_c$ can be expressed as follows:

$$Q = A U_{\mathrm{III}} t_{\mathrm{III}} (\overline{T}_b - \overline{T}_c) \tag{23}$$

where $A$ is the cooling surface area, $U_{\mathrm{III}}$ the overall heat transfer coefficient in freezing stage, $t_{\mathrm{III}}$ the period of freezing during which ice is formed, $\overline{T}_b$ is the bulk solution temperature, which is equal to the freezing point $T_f$ of the juice because the system was in phase equilibrium, i.e., $T_b = T_f$, and $T_{\mathrm{c}}$ is the refrigerant temperature. Both $T_{\mathrm{b}}$ and $T_{\mathrm{c}}$ decreased linearly, so the average values were use in Eq. (23).

By energy conservation, the release of latent heat of freezing was equal to the heat carried away by the refrigerant, so the overall heat transfer coefficient can be expressed as follows (Qin et al., 2006):

$$U_{\mathrm{III}} = \frac{M_{j0}\Delta H}{A t_{\mathrm{III}}(\overline{T}_b - \overline{T}_c)}\left(1 - \frac{C_{j0}}{C_{j1}}\right) = \frac{w\Delta H}{A(\overline{T}_b - \overline{T}_c)} \tag{24}$$

Thus, the value of the overall heat transfer coefficient $U_{III}$ could be experimentally obtained by measuring the juice concentration before and after FC, i.e., $C_{j0}$ and $C_{j1}$, the freezing time $t_{III}$, and the temperature difference between the bulk solution and refrigerant ($\overline{T}_b - \overline{T}_c$). This equation is also applicable for the overall heat transfer coefficients of passes 2 and 3 if the juice masses, freezing times, and juice concentrations before and after FC of passes 2 and 3 are substituted in the equation.

## 4. Experimental results and discussion

### 4.1. Ice production rate and heat transfer coefficient

To acquire information about the heat and mass transfer of the screw-scraper SSHE with and/or without phase change, published experimental data were re-used in this study, as shown in Fig. 3. During the FC of apple juice in pass 1, the juice temperature dropped without phase change in stage I from the beginning of the process to 7500 s. This was followed by stage II, in which the onset of the phase change occurred, and the juice temperature jumped from undercooling to its phase equilibrium temperature (i.e., the freezing point) because the latent heat of freezing was released by the ice crystals. Stage III was a steady-state period of FC (ice production stage) during which the juice concentration increased gradually. The juice concentration could be calculated based on the freezing point temperature of the juice and plotted on the screen in real-time, as shown by the red curve in Fig. 3.

One of the main parameters that characterizes the performance of an SSHE is its heat transfer coefficient $U$, and the parameter that characterizes its mass transfer is the ice production rate $w$. During the FC process, the heat transfer of the SSHE was divided into two stages: the heat transfer coefficient $U_{\mathrm{I}}$ of the cooling stage (Stage I) and the heat transfer coefficient $U_{\mathrm{III}}$ of the freezing stage (including Stages II and III).

In the cooling stage, by measuring (1) the temperature drop of the apple juice, (2) the temperature difference between the fruit juice and refrigerant, and (3) the mass of apple juice (obtained by weighing) and by setting the rotation speed of the SSHE to 60 rpm, the heat transfer coefficient $U_{\mathrm{I}}$ of the SSHE was obtained by Eq. (21). The experimental results are shown in Table 2, in which the original apple juice concentration was $C_{\mathrm{j0}} = 10.5$ °Bx, density $\rho = 1.04098$ kg $L^{-1}$ (Constenla et al., 1989), volume $V = 3.0$ L, weight $M_{\mathrm{j0}} = 3.123$ kg, and specific heat capacity $c_{\mathrm{p}} = 3.94$ kJ $kg^{-1}$ °$C^{-1}$ (Magerramov, 2007).

In the freezing stage (Stages II and III), the ice production and heat transfer coefficient were correlated with the concentration change of the fruit juice. The ice production rate $w$ and heat transfer coefficient $U_{\mathrm{III}}$ were obtained from Eqs. (19) and (24), respectively, using experimental data. The measurement results are shown in Table 3. From these results, the following were determined:

(1) The heat transfer coefficient and ice production capacity of the SSHE decreased with the increase in the juice concentration. Nevertheless, compared with heat transfer coefficient of the progressive crystallization FC, which is normally less than 0.1 kJ $m^{-2}$ °$C^{-1}$ (Qin et al., 2003a; Pronk et al., 2010; Hasan et al., 2017), the heat transfer coefficient of the suspension crystallization FC found in this experiment was 3–6 times higher.
(2) The data in Tables 2 and 3 show that the heat transfer coefficient $U_{\mathrm{III}}$ of the freezing stage (with phase change) had a step increase of 1.32–2.35 times the heat transfer coefficient $U_{\mathrm{I}}$ of the cooling stage (without phase change).

**Table 2**
Three sets of experimental measurements of the heat transfer coefficient ($U_I$) of the SSHE during the cooling stage (stage I).

| Exp. group | | No. | $C_{j0}$ °Bx | $M_j$ (kg) | $T_{b1}$ (°C) | $T_{b2}$ (°C) | $T_c$ (°C) | $t_I$ (s) | $U_I$ kW m$^{-2}$ °C$^{-1}$ |
|---|---|---|---|---|---|---|---|---|---|
| ① | Pass 1 | 1 | 10.50 | 3.12 | 28.90 | −1.10 | −4.80 | 4050 | 0.22 |
| | Pass 2 | 2 | 18.60 | 1.19 | 29.90 | −2.20 | −4.60 | 2097 | 0.20 |
| | Pass 3 | 3 | 26.80 | 0.56 | 30.20 | −3.80 | −4.40 | 1410 | 0.21 |
| ② | Pass 1 | 4 | 10.50 | 3.12 | 29.80 | −1.10 | −3.90 | 3798 | 0.26 |
| | Pass 2 | 5 | 20.30 | 1.20 | 27.80 | −2.50 | −4.40 | 1854 | 0.23 |
| | Pass 3 | 6 | 27.90 | 0.56 | 28.00 | −4.10 | −4.70 | 1332 | 0.21 |
| ③ | Pass 1 | 7 | 10.50 | 3.12 | 28.50 | −1.10 | −4.30 | 4158 | 0.22 |
| | Pass 2 | 8 | 19.20 | 1.20 | 28.00 | −2.30 | −4.70 | 1845 | 0.22 |
| | Pass 3 | 9 | 26.70 | 0.56 | 29.40 | −3.80 | −4.10 | 1398 | 0.24 |
| | Ave. of pass 1 | | 10.50 ± 0.00 | | | | | 4002 | 0.23 ± 0.03 |
| | Ave. of pass 2 | | 19.40 ± 0.90 | | | | | 1932 | 0.21 ± 0.02 |
| | Ave. of pass 3 | | 27.10 ± 0.90 | | | | | 1380 | 0.22 ± 0.02 |

Note: (1) the crystallizer volume for pass 1 = 3 L, pass 2 = 1.1 L, and pass 3 = 0.5 L; the cooling surface area $A = 0.0314$ m$^2$; (2) the specific heat capacity of the apple juice (referring to the same concentration of sucrose solution) $c_p = 3.94$ kJ kg$^{-1}$ °C$^{-1}$; (3) the rotational speed of the SSHE was 60 rpm; and (4) ①, ②, and ③ represent the three sets of experiments.

**Table 3**
Three sets of experimental measurements of the heat transfer coefficient ($U_{III}$) and ice production rate ($w$) of the SSHE during the freezing stage (Stages II and III).

| Exp. group | | No. | $C_{j0}$ °Bx | $C_{j1}$ °Bx | $M_j$ (kg) | $\overline{T}_b$ (°C) | $\overline{T}_c$ (°C) | $M_i$ (kg) | $t_{III}$ (s) | $U_{III}$ kW m$^{-2}$ °C$^{-1}$ | $w$ kg h$^{-1}$ m$^{-2}$ |
|---|---|---|---|---|---|---|---|---|---|---|---|
| ① | Pass 1 | 1 | 10.50 | 18.60 | 3.12 | −1.70 | −6.30 | 1.36 | 6042 | 0.52 | 25.80 |
| | Pass 2 | 2 | 18.60 | 26.80 | 1.19 | −3.04 | −6.90 | 0.36 | 2475 | 0.41 | 15.92 |
| | Pass 3 | 3 | 26.80 | 34.50 | 0.56 | −4.89 | −7.40 | 0.12 | 1755 | 0.30 | 7.96 |
| ② | Pass 1 | 4 | 10.50 | 20.30 | 3.12 | −1.72 | −6.50 | 1.51 | 5740 | 0.58 | 30.25 |
| | Pass 2 | 5 | 20.30 | 27.90 | 1.20 | −3.32 | −7.7 | 0.33 | 1752 | 0.45 | 21.34 |
| | Pass 3 | 6 | 27.90 | 35.70 | 0.56 | −5.22 | −8.1 | 0.12 | 1559 | 0.29 | 8.92 |
| ③ | Pass 1 | 7 | 10.50 | 19.20 | 3.12 | −1.74 | −7.00 | 1.41 | 5381 | 0.54 | 30.57 |
| | Pass 2 | 8 | 19.20 | 26.70 | 1.20 | −3.08 | −8.00 | 0.34 | 1613 | 0.45 | 23.89 |
| | Pass 3 | 9 | 26.70 | 36.80 | 0.56 | −5.26 | −9.10 | 0.15 | 1524 | 277 | 11.46 |
| | Ave. of pass 1 | | 10.50 ± 0.00 | 19.40 ± 0.90 | | | | | 5721 | 0.54 ± 0.03 | 28.66 ± 1.59 |
| | Ave. of pass 2 | | 19.40 ± 0.90 | 27.10 ± 0.90 | | | | | 1947 | 0.44 ± 0.02 | 20.38 ± 3.50 |
| | Ave. of pass 3 | | 27.10 ± 0.90 | 35.70 ± 1.10 | | | | | 1613 | 0.29 ± 0.01 | 9.55 ± 1.91 |

Notes: juice mass $M_j$ was determined by weighing.

For every stage, the interval averages are shown in Tables 2 and 3 because the instantaneous heat transfer coefficient and ice production rate could not be measured directly. Based on comprehensive analysis of the results shown by Table 2 (Stage I of heat transfer) and Table 3 (Stages II and III of heat transfer), the step changes of the heat transfer coefficient from $U_I$ *to* $U_{III}$ and the ice production rate $w$ are illustrated in Fig. 4. Tracking the change of the heat transfer coefficient $U$ and ice production rate $w$ during the pass-1 FC, i.e., the black lines in Fig. 4, it is evident that the pass-1 FC had higher values of the heat transfer coefficient (black dotted line) and ice production rate (black solid line) than those of passes 2 and 3. Both the heat transfer coefficient (dotted lines) and ice production rate (solid lines) decreased stepwise in pass 2 (red) and pass 3 (blue). The results showed that with the increase in the fruit juice concentration, the soluble solid (solute), as an impurity for ice crystallization, increasingly hindered the growth of ice crystals. In other words, the increase in the mass transfer resistance gradually restricted the process of heat transfer.

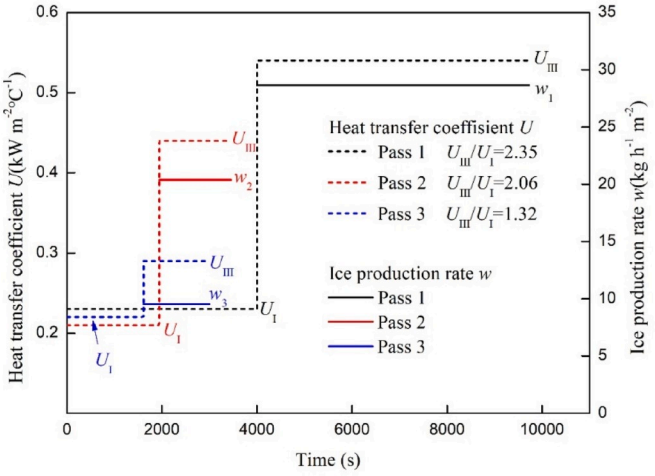


**Fig. 4.** Experimental values of the heat transfer coefficient ($U$) and ice production rate ($w$) of the system in Stages I, II, and III.

### 4.2. Influence of SSHE rotation speed

When analyzing and modeling the heat and mass transfer of the SSHE, as given by Eqs. (1) and (2), the scraper not only destroyed the flow boundary layer of the juice on the cooling surface in the cooling stage (stage I) to enhance the heat transfer, but it also scraped off the ice layer adhering to the cooling surface in the freezing stage (Stages II and III) and improved the heat and mass transfer effects. However, we ignored the friction effect between the scraper and cooling surface, which generated frictional heat to counteract the cooling of the refrigeration unit more or less. Higher rotational speeds produced more frictional heat. By changing the rotational speed $n$ but keeping the juice initial concentration the same, the effects of the rotational speed $n$ on the performance metrics of the apparatus, such as the cooling and freezing rates, were investigated. The experimental results are shown in Table 4. The SSHE and crystallizer had the best heat and mass transfer effects when the scraper was set to the lowest speed of 60 rpm. Although an even lower speed than that might has a better cooling effect according to the trend showing in Table 4, it was the minimum speed that could be set by the experimental device. Therefore, further experiments with

**Table 4**
Effect of the rotational speed of the scraper on the performance of SSHE.

| n rpm | R °C h$^{-1}$ | $P_I$ kW | $U_I$ kJ m$^{-2}$ °C$^{-1}$ | $U_{III}$ kJ m$^{-2}$ °C$^{-1}$ | w kg h$^{-1}$ m$^{-2}$ | W kW h kg$^{-1}$ |
|---|---|---|---|---|---|---|
| 60 | 25.30 | 0.091 | 0.215 | 0.520 | 25.89 | 0.318 |
| 100 | 17.71 | 0.064 | 0.216 | 0.503 | 24.30 | 0.326 |
| 125 | 17.59 | 0.060 | 0.206 | 0.482 | 23.22 | 0.329 |
| 150 | 16.83 | 0.057 | 0.203 | 0.480 | 22.45 | 0.340 |
| 175 | 16.69 | 0.057 | 0.201 | 0.463 | 21.91 | 0.348 |
| 200 | 16.26 | 0.056 | 0.206 | 0.477 | 20.67 | 0.369 |
| 225 | 15.66 | 0.053 | 0.189 | 0.412 | 17.42 | 0.438 |
| 250 | 15.61 | 0.053 | 0.185 | 0.404 | 18.41 | 0.415 |

Note: $n$ = rotation speed of the scraper, $R$ = cooling rate in stage I, $P_I$ = cooling capacity of the refrigeration unit in the cooling stage, $U_I$ = heat transfer coefficient of the SSHE in the cooling stage, $U_{III}$ = heat transfer coefficient in the freezing stage, $w$ = ice production rate, and W = energy consumption of ice production.

reduced rotational speeds must be carried out after improving the equipment.

The measured data of the power allocation of the main components in the freeze concentrator are shown in Table 5. The largest power consumption of the system was the refrigeration unit, followed by the drive motor of the scraper heat exchanger. The actual power consumption of both was less than the nominal power consumption, which indicated that they operated normally. The power consumption of other components was relatively small and had little impact on the power consumption of the whole machine.

### 4.3. Concentration ratio (r), partition coefficient (p), recovery yield (y), and crystallinity of juice (f)

In this study, the apple juice was concentrated with multi-pass FC, and its concentration increased step by step in three passes. The experimental data is shown in Table 6, where the apple juice initial concentration was $C_{j0}$ = 10.5°Bx, the density was $\rho$ = 1.04098 kg L$^{-1}$, the volume was $V$ = 3.0 L, the mass was $M_j$ = 3.123 kg, and the specific heat was $c_p$ = 3.94 kJ kg$^{-1}$ °C$^{-1}$. The analysis and calculation of the concentration ($C$), concentration ratio ($r$), partition coefficient ($p$), mass fraction of ice ($f$), and recovery yield ($y$) of soluble solid, which were all correlated to the heat and mass transfer of the SSHE, are presented in Section 3 of this paper.

In suspension crystallization FC, the value of the partition coefficient $p$ is usually small due to the small amount of solute entrainment in the ice, as shown in Table 6. Moreover, it was interesting that in the three stages from pass 1 to 3, the higher heat transfer and ice production rates seemed to not lead to a higher partition coefficient $p$, i.e., higher solute entrainment in the ice. On the contrary, when the rates of heat and mass transfer (ice production) were high, the solute entrainment was low. Table 6 also shows that the concentration ratio $r$ decreased with the increase in the number of FC passes, namely, the FC efficiency decreased with the increase in the juice concentration. This might be attributed to the solute of the juice as impurities of the ice crystals, which behaved as an inhibitor to ice crystal growth, preventing Ostwald ripening. The effect became stronger with the increase in the juice concentration.

**Table 5**
Energy consumption of the main components of the instrument.

| Components | $P_{Nom}$ (kW) | $P_{Tes}$ (kW) | $P_{Nom}/P_{Tes}$ |
|---|---|---|---|
| Driving motor | 0.120 | 0.081 | 67.5% |
| Refrigeration unit | 0.150 | 0.123 | 82% |
| Control unit and touch screen | 0.025 | 0.025 | 100% |
| Solenoid valves (1) | 0.05 | 0.05 | 100% |
| Pump | 0.010 | 0.010 | 100% |
| Total | 0.355 | 0.289 | 81.4% |

Notes: (1) solenoid valves operated only in feeding and discharging periods, otherwise they had no power consumption. (2) $P_{Nom}$ = nominal power consumption, and $P_{Tes}$ = tested power consumption.

The scientific definition of the partition coefficient $p$ is the ratio of the soluble solid content of the ice crystal ($C_i$) to that of mother solution, i.e., concentrated juice ($C_j$) when ice crystallizes in the state of near phase equilibrium with the solution (juice) (Lide and Haynes, 2010). This requires $\Delta T$ and $\Delta C$ for heat and mass transfer to be very small to eliminate the concentration polarization. However, when the juice concentration increases, its viscosity increases consequently, which hinders the heat and mass transfer as well. To maintain the ice crystallization, a larger temperature difference ($\Delta T$) for freezing would be applied, which would cause the system to deviate from the phase equilibrium state. Moreover, as the juice viscosity increases, after the separation of the ice and juice, the adhesion of the thickened juice on the ice surface rather than distributing inside the ice crystals would be the major reason for solute entrainment by the ice. Therefore, the measured values of $p$ were no longer the true values of partition coefficient but became slightly greater as the juice concentration increased, and also known as the effective partition coefficient (Miyawaki et al., 2005), as shown in Table 6.

In progressive crystallization, droplets or solutes are occluded in the ice. According to Miyawaki et al., the $p$ value of progressive FC depends on the solution type, concentration, and flow rate of the solution. Thicker solutions lead to higher $p$ values. When the concentration of pure sucrose solution is ~8%, the flow rate of the solution is 3.42–4.79 m s$^{-1}$, the growth rate of ice crystals is 8.75–9.54 mm h$^{-1}$, and the partition coefficient $p$ is between 0.142 and 0.289 (Miyawaki et al., 2005). This was slightly lower than the data reported by Chen et al. (Chen and Chen, 2000). To reduce the solid solute loss caused by the ice entraining the mother liquor in progressive crystallization FC, Gunathilake and Miyawaki explored the technique of thawing a small portion of the ice and then adding it back into the concentrate. The result showed that when the concentration of apple juice increased from 13.7 to 25.5°Br, and the recovery yield of the soluble solid increased from 63.8% to 85% (Gunathilake et al., 2014). Samsuri et al. proposed a progressive crystallization FC method using spiral-finned tubes as the cooling surface and optimized the process conditions with response surface methodology. The values of the partition coefficient $p$ were between 0.17 and 0.3, which were basically greater than 0.2 (Moreno et al., 2014c). In general, the values of the partition coefficient $p$ of the suspended crystallization FC obtained in this study were significantly smaller than those of progressive FC and Block FC.

## 5. Conclusion

In this study, mathematical models for heat and mass transfer of FC by suspension crystallization revealed that there was a step increase of the heat flux at the scraped cooling surface after phase change (freezing) occurred. The feasibility of the model was verified in a three-pass suspension freeze concentrator. The concentration ratios before and after FC and the partition coefficient of solute in the ice crystals and mother liquor, which characterized the solute entrainment in ice, were measured and correlated with the corresponding ice production rate. A higher ice production rate did not necessarily lead to more solute entrainment, but it was related to the concentration and viscosity of the mother liquor.

## CRediT authorship contribution statement

**Zhongxiang Ding:** Investigation, Data curation, Formal analysis, Visualization, Writing - original draft. **Frank G.F. Qin:** Conceptualization, Funding acquisition, Formal analysis, Supervision, Writing - review & editing. **Kewen Peng:** Data curation, Software, Validation. **Jiaojiao Yuan:** Methodology. **Simin Huang:** Investigation. **Runhua Jiang:** Software. **Youyuan Shao:** Methodology.

**Table 6**
Correlation of heat and mass transfer with the concentration ratio, partition coefficient, mass fraction of ice, and recovery yield in multi-pass FC process.

| | $U_{III}$ kW m$^{-2}$ °C$^{-1}$ | w kg h$^{-1}$ m$^{-2}$ | $C_{j0}$ °Bx | $C_{j1}$ °Bx | $C_i$ °Bx | r | p | f | y |
|---|---|---|---|---|---|---|---|---|---|
| Pass 1 | 0.54 ± 0.03 | 28.66 ± 1.59 | 10.5 | 18.6 | 0.15 | 1.77 | 0.0081 | 0.435 | 0.996 |
| Pass 2 | 0.44 ± 0.02 | 20.38 ± 3.50 | 18.6 | 26.8 | 0.24 | 1.44 | 0.027 | 0.360 | 0.990 |
| Pass 3 | 0.29 ± 0.01 | 9.55 ± 1.91 | 26.8 | 34.5 | 2.31 | 1.32 | 0.067 | 0.223 | 0.985 |

Note: the heat transfer coefficient $U_{III}$ and ice production rate $w$ were the average values of the three repeated experiments listed in the last three rows of Table 3.

## Acknowledgments

The authors would like to acknowledge the financial sponsorship of the National Key R&D Program of China (2016YFD04003032) and the NNSFC (21376052).

## References

Abichandani, H., Sarma, S., Heldman, D., 1987. Hydrodynamics and heat transfer in liquid full scraped surface heat exchangers: a review. J. Food Process. Eng. 9, 121.
Bayindirli, L., Ozilgen, M., Ungan, S., 1993. Mathematical analysis of freeze concentration of apple juice. J. Food Eng. 19, 95–107.
Benedetti, S., Prudêncio, E.S., Nunes, G.L., Guizoni, K., Fogaça, L.A., Petrus, J.C.C., 2015. Antioxidant properties of tofu whey concentrate by freeze concentration and nanofiltration processes. J. Food Eng. 160, 49–55.
Chen, P., Chen, X.D., 2000. A generalized correlation of solute inclusion in ice formed from aqueous solutions and food liquids on sub-cooled surface. Can. J. Chem. Eng. 78 (2), 312–319.
Constenla, D.T., Lozano, J.E., Crapiste, G.H., 1989. Thermophysical properties of clarified apple juice as a function of concentration and temperature. J. Food Sci. 54 (3), 66–71.
Ding, Z., Qin, F.G.F., Yuan, J., Huang, S., Jiang, R., Shao, Y., 2019. Concentration of apple juice with an intelligent freeze concentrator. J. Food Eng. 256, 61–72.
Gunathilake, M., Dozen, M., Shimmura, K., Miyawaki, O., 2014. An apparatus for partial ice-melting to improve yield in progressive freeze-concentration. J. Food Eng. 142, 64–69.
Habib, B., Farid, M., 2007. Freeze concentration of milk and saline solutions in a liquid-solid fluidized bed Part I. Experimental. Chemical Engineering and Processing: Process Intensification 46, 1400–1411.
Hasan, M., Filimonov, R., Chivavava, J., Sorvari, J., Louhi-Kultanen, M., Lewis, A.E., 2017. Ice growth on the cooling surface in a jacketed and stirred eutectic freeze crystallizer of aqueous $Na_2SO_4$ solutions. Separ. Purif. Technol. 175, 512–526.
Huige, N.J.J., Thijssen, H.A.C., 1972. Production of large crystals by continuous ripening in a stirrer tank. J. Cryst. Growth 13/14, 483–487.
Lide, D.R., Haynes, W.M. (Eds.), 2010. CRC Handbook of Chemistry and Physics, 90th ed. CRC Press.
Magerramov, M.A., 2007. Heat capacity of natural fruit juices and of their concentrates at temperatures from 10 to 120°C. J. Eng. Phys. Thermophys. 80 (5), 1055–1063.
Miyawaki, O., Liu, L., Shirai, Y., Sakashita, S., Kagitani, K., 2005. Tubular ice system for scale-up of progressive freeze-concentration. J. Food Eng. 69 (1), 107–113.
Miyawaki, O., Gunathilake, M., Omote, C., Koyanagi, T., Sasaki, T., Take, H., Matsuda, A., Ishisaki, K., Miwa, S., Kitano, S., 2016a. Progressive freeze-concentration of apple juice and its application to produce a new type apple wine. J. Food Eng. 171, 153–158.
Miyawaki, O., Omote, C., Gunathilake, M., Ishisaki, K., Miwa, S., Tagami, A., Kitano, S., 2016b. Integrated system of progressive freeze-concentration combined with partial ice-melting for yield improvement. J. Food Eng. 184, 38–43.
Moreno, F.L., Hernández, E., Raventós, M., Robles, C., Ruiz, Y., 2014a. A process to concentrate coffee extract by the integration of falling film and block freeze-concentration. J. Food Eng. 128 (1), 88–95.
Moreno, F.L., Raventós, M., Hernández, E., Ruiz, Y., 2014b. Block freeze-concentration of coffee extract: effect of freezing and thawing stages on solute recovery and bioactive compounds. J. Food Eng. 120 (1), 158–166.
Moreno, F.L., Raventós, M., Hernández, E., Ruiz, Y., 2014c. Block freeze-concentration of coffee extract: effect of freezing and thawing stages on solute recovery and bioactive compounds. J. Food Eng. 120, 158–166.
Orellana-Palma, P., Petzold, G., Torres, N., Aguilera, M., 2017. Elaboration of orange juice concentrate by vacuum-assisted block freeze concentration. J. Food Process. Preserv. 42 (2).
Petzold, G., Niranjan, K., Aguilera, J.M., 2013. Vacuum-assisted freeze concentration of sucrose solutions. J. Food Eng. 115 (3), 357–361.
Pronk, P., Infante Ferreira, C.A., Witkamp, G.J., 2005. A dynamic model of Ostwald ripening in ice suspensions. J. Cryst. Growth 275, e1355–e1361.
Pronk, P., Ferreira, C.A.I., Witkamp, G.J., 2010. Mitigation of ice crystallization fouling in stationary and circulating liquid–solid fluidized bed heat exchangers. Int. J. Heat Mass Tran. 53, 403–411.
Qin, F.G.F., Russell, A.B., Chen, X.D., Robertson, L., 2003a. Ice fouling on a subcooled metal surface examined by thermo-response and electrical conductivity. J. Food Eng. 59, 421–429.
Qin, F.G.F., Chen, X.D., Russell, A.B., 2003b. Heat transfer at the subcooled-scraped surface with/without phase change. AIChE J. 49 (8), 1947–1955.
Qin, F.G.F., Chen, X.D., Farid, M.M., 2004. Growth kinetics of ice films spreading on a subcooled solid surface. Separ. Purif. Technol. 39, 109–121.
Qin, F.G.F., Chen, X.D., Ramachandra, S., Free, K., 2006. Heat transfer and power consumption in a scraped-surface heat exchanger while freezing aqueous solutions. Separ. Purif. Technol. 48, 150–158.
Qin, F.G.F., Premathilaka, S., Chen, X.D., Free, K.W., 2007. The shaft torque in a laboratory scraped surface heat exchanger used for making ice slurries. In: Asia-Pacific Journal of Chemical Engineering, vol. 2. Curtin University of Technology and John Wiley & Sons, Ltd.), pp. 618–630.
Qin, F.G.F., Chen, X.D., Premathilaka, S., Free, K.W., 2008. Experimental study of wash columns used for separating ice from ice-slurry. Desalination 218, 223–228.
Qin, F.G.F., Yang, M.L., Yang, X.X., Chen, X.D., Abeynaike, A., 2009a. Experimental and thermal analysis of washing the packed ice bed in wash columns. AIChE J. 55 (11), 2835–2847.
Qin, F.G.F., Chen, X.D., Free, K.W., 2009b. Freezing on subcooled surfaces, phenomena, modeling and applications. Int. J. Heat Mass Tran. 52, 1245–1253.
F.G.F. Qin, L. Tu, J. Yuan, Experimental study of a pilot scale freeze concentration unit, in The Food Factor I Barcelona Conference. 2-4 November 2016: Barcelona, Spain.
Qin, F.G.F., Ding, Z., Yuan, J., Huang, S., Jiang, R., Shao, Y., 2019. Visualization data on concentrating apple juice with a trinitarian crystallization suspension freeze concentrator. Data in Brief 26 (Summar), 104255.
Randall, D.G., Nathoo, J., 2015. A succinct review of the treatment of Reverse Osmosis brines using Freeze Crystallization. Journal of Water Process Engineering 8, 186–194.
Rao, C.S., Hartel, R.W., 2006. Scraped surface heat exchangers. Crit. Rev. Food Sci. Nutr. 46 (3), 207–219.
Samsuri, S., Amran, N.A., Jusoh, M., 2015. Spiral finned crystallizer for progressive freezeconcentration process. Chem. Eng. Res. Des. 104, 280–286.
Sanchez, J., Hernandez, E., Auleda, J.M., Raventos, M., 2011. Review: freeze concentration technology applied to dairy products. Food Sci. Technol. Int. 17 (1), 5–13.
Schwartzberg, H.G., 1990. Food freeze concentration. In: Rao, M.A., Schwartzberg, H.G. (Eds.), Biotechnology and Food Process Engineering. Marcel Dekker, New York.
Thijssen, H., 1974. Freeze concentration. In: Spicer, A. (Ed.), Advances in Preconcentration and Dehydration of Foods. Wiley, pp. 115–149.
Zambrano, A., Ruiz, Y., Hernández, E., Raventós, M., Moreno, F.L., 2018. Freeze desalination by the integration of falling film and block freeze-concentration techniques. Desalination 436, 56–62.